Research Paper

7-O-Esters of taxifolin with pronounced and overadditive effects in neuroprotection, anti-neuroinflammation, and amelioration of short-term memory impairment *in vivo*

Sandra Gunesch[a], Matthias Hoffmann[a], Carolina Kiermeier[a], Wolfgang Fischer[b], Antonio F.M. Pinto[b], Tangui Maurice[c], Pamela Maher[b],**, Michael Decker[a],*

[a] *Pharmaceutical and Medicinal Chemistry, Institute of Pharmacy and Food Chemistry, Julius Maximilian University of Würzburg, Am Hubland, 97074, Würzburg, Germany*
[b] *The Salk Institute for Biological Studies, 10010 N Torrey Pines Road, La Jolla, CA, 92037, USA*
[c] *MMDN, University of Montpellier INSERM, EPHE, UMR-S1198, 434095, Montpellier, France*

ARTICLE INFO

ABSTRACT

Alzheimer's disease (AD) is a multifactorial disease and the most common form of dementia. There are no treatments to cure, prevent or slow down the progression of the disease. Natural products hold considerable interest for the development of preventive neuroprotectants to treat neurodegenerative disorders like AD, due to their low toxicity and general beneficial effects on human health with their anti-inflammatory and antioxidant features. In this work we describe regioselective synthesis of 7-O-ester hybrids of the flavonoid taxifolin with the phenolic acids cinnamic and ferulic acid, namely 7-O-cinnamoyltaxifolin and 7-O-feruloyltaxifolin. The compounds show pronounced overadditive neuroprotective effects against oxytosis, ferroptosis and ATP depletion in the murine hippocampal neuron HT22 cell model. Furthermore, 7-O-cinnamoyltaxifolin and 7-O-feruloyltaxifolin reduced LPS-induced neuroinflammation in BV-2 microglia cells as assessed by effects on the levels of NO, IL6 and TNFα. In all *in vitro* assays the 7-O-esters of taxifolin and ferulic or cinnamic acid showed strong overadditive activity, significantly exceeding the effects of the individual components and the equimolar mixtures thereof, which were almost inactive in all of the assays at the tested concentrations. *In vivo* studies confirmed this overadditive effect. Treatment of an AD mouse model based on the injection of oligomerized Aβ$_{25-35}$ peptide into the brain to cause neurotoxicity and subsequently memory deficits with 7-O-cinnamoyltaxifolin or 7-O-feruloyltaxifolin resulted in improved performance in an assay for short-term memory as compared to vehicle and mice treated with the respective equimolar mixtures. These results highlight the benefits of natural product hybrids as a novel compound class with potential use for drug discovery in neurodegenerative diseases due to their pharmacological profile that is distinct from the individual natural components.

1. Introduction

Currently, 50 million people live with dementia and about two thirds of them suffer from Alzheimer's disease (AD), making AD the most common form of dementia with numbers expected to increase dramatically due to our aging society [1]. So far, only 4 of more than 100 attempts to develop a drug against AD have resulted in a product on the market. Moreover, the available drugs only alleviate symptoms and are not able to stop neurodegeneration or cure the disease [1]. Advances in AD drug development have been hampered for several reasons with most of the researchers focused on amyloid β as the main perpetrator for AD [2]. Abnormal protein aggregation of amyloid β accumulating as extracellular plaques in the brain, and hyperphosphorylated tau protein forming neurofibrillary tangles are the main characteristics of AD, but neuroinflammation and oxidative stress are just as important as hallmarks of the disease and contribute dramatically to its progression [3]. Due to the multifactorial nature of AD, the one-target strategy to fight the disease needs to be replaced by a more general approach using pleiotropic compounds to deal with its complexity.

Natural products such as flavonoids are used as active components of natural remedies for the treatment of various diseases in traditional

---

medicine. Their well-established antioxidant features proved to be beneficial for general human health and natural products have gained increased attention with respect to their potential as neuroprotectants, as by their nature they show pleiotropic effects instead of addressing a single target [4,5].

In previous work we used the natural product silibinin to synthesize a library of 7-O-esters of this flavonolignan with different phenolic acids and investigated their neuroprotective features in a set of assays related to neurodegeneration and aging [6]. The library of esters of silibinin with derivatives of ferulic acid, using substituted and un-substituted cinnamic, dihydro cinnamic and benzoic acids was investigated for structure-activity relationships (SARs) to reveal the influence of different numbers of hydroxy- and methoxy-groups as aromatic substituents as well as the Michael system on the neuroprotective and antioxidant effects. In all cases, we used natural products or simple derivatives thereof. SARs analysis showed that phenolic acids possessing a Michael system are important for the neuroprotective activity of the compounds [6]. The assays applied were cell-based, avoiding potentially false positive results due to false positive readouts as it was shown for pan assay interference compounds (PAINS) [7,8]. The most potent esters of the compound library in that study were 7-O-cinnamoylsilibinin and 7-O-feruloylsilibinin. Phenolic acids have been studied in the context of neurodegenerative diseases before due to their antioxidant capacities. Ferulic acid is a free radical scavenger which can counteract apoptotic intracellular pathways induced by oxidative stress [9], and has been studied in *in vivo* models of AD. Long-term administration of ferulic acid counteracted the neurotoxic effect induced by amyloid β in mice [10] and reduced behavioral impairment in a transgenic PSAPP mouse model [11]. Cinnamic acid upregulated the suppressor of cytokine signaling 3 (SOCS3) in BV-2 microglial cells and suppressed the expression of pro-inflammatory cytokines counteracting neuroinflammation [12].

Flavonolignan-based silibinin-esters with phenolic acids suffer from some drawbacks. The high molecular weight of the compounds and their constrained solubility counteract their drugability [13]. The secondary plant metabolite taxifolin is a flavonoid, structurally closely related to silibinin, but smaller in size (Fig. 1). In addition, the catechol moiety in taxifolin is an important antioxidant group itself and it has

been shown to site-specifically inhibit aggregation of 42-residue amyloid β-protein (Aβ42) *in vitro*, which is relevant for the pathogenesis of AD. [14] This was confirmed by a computational study analyzing the reaction mechanism. The covalent adduct is formed via an aza-Michael addition of the oxidized *o*-quinone species of (+)-taxifolin with a lysine residue of the Aβ42 fibril [15]. Previously, taxifolin was semi-synthetically esterified in position 7 with gallic acid by Vrba et al. and shown to upregulate the nuclear factor (erythroid-derived 2)-like 2 (Nrf2) pathway in RAW264.7 cells [16], an important cytoprotective mechanism in response to redox imbalance. Recently, it has been shown that orally administered taxifolin exhibits a pleiotropic beneficial effect on intracerebral profiles in a cerebral amyloid angiopathy (CAA) mouse model *in vivo*, a disease often accompanied by AD [17]. By highlighting the therapeutic potentials of taxifolin and the phenolic acids ferulic and cinnamic acid in the context of neurodegenerative diseases [18,19], these findings inspired us to investigate natural product hybrids based on the flavonoid taxifolin and phenolic acids as novel potent neuroprotectants.

Thus, we present in this paper studies on the 7-O-esters of taxifolin with the phenolic acids cinnamic and ferulic acid (Fig. 1B). The latter had proven to be the most effective acids in a comprehensive medicinal chemical structure-activity relationships (SARs) study with silibinin besides their individual neuroprotective features as outlined above. The 7-O-taxifolin esters were regioselectively synthesized without the need of protective groups using acyl chlorides [6,16]. To target AD as a multi-factorial disease with age being the highest risk factor, the compounds need to have a broad pharmacological profile. We assessed the compounds' neuroprotective effects using different cellular models reflecting neurodegeneration and the biology of the aging brain [20]. The hybrids 7-O-cinnamoyltaxifolin **1** and 7-O-feruloyltaxifolin **2** were investigated using the mouse hippocampal neuronal cell line HT22 in different assays of oxidative stress-induced cell death and mouse BV-2 microglia cells for the protection against neuroinflammation. Cellular uptake experiments demonstrated the stability of the compounds under cell culture conditions. Additionally, **1** and **2** were investigated *in vivo* in an AD mouse model which showed their protective effects towards Aβ_{25-35}-induced memory impairment [21].
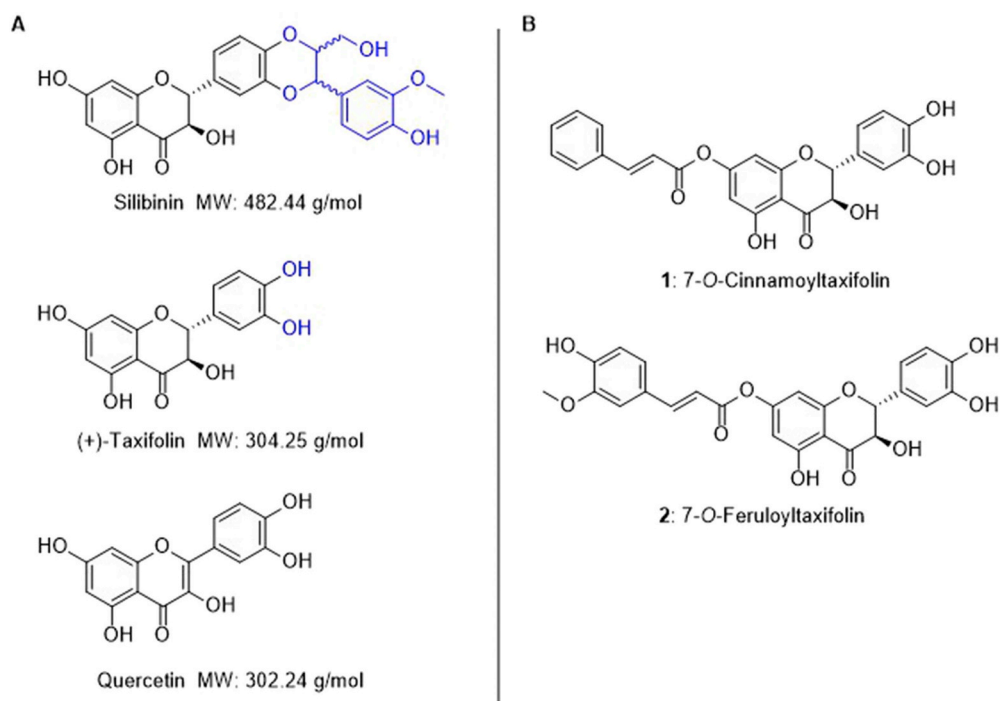

Fig. 1. **A**) Chemical structures of the flavonolignan silibinin and the flavonoids taxifolin and quercetin. Structural differences between the natural products silibinin and taxifolin are highlighted in blue. **B**) Target compounds 7-O-cinnamoyltaxifolin (**1**) and 7-O-feruloyltaxifolin (**2**). (For interpretation of the references to color in this figure legend, the reader is referred to the Web version of this article.)
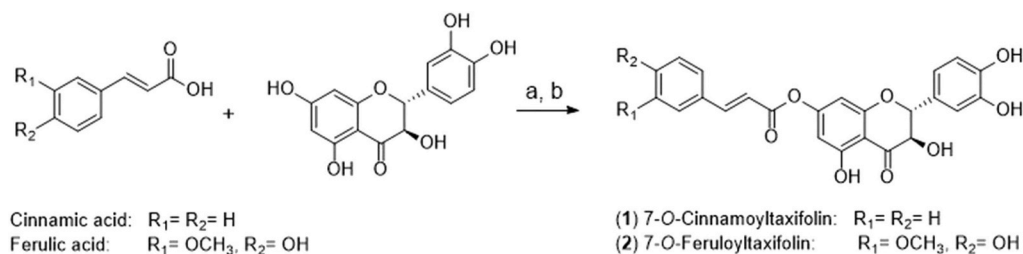
Scheme 1. Synthesis of 7-*O*-cinnamoyltaxifolin (**1**, 43% yield) and 7-*O*-feruloyltaxifolin (**2**, 27% yield). a) acid, oxalyl chloride, DMF, dry THF, 1 h, room temperature; b) taxifolin, triethylamine, dry THF, 2 h, room temperature after addition of the respective acyl chloride.

2. Results

Chemistry. Despite the presence of several hydroxyl groups, 7-*O*-esterification of taxifolin was achieved without the use of protective groups under optimized reaction conditions. Acyl chlorides of ferulic or cinnamic acid were generated with oxalyl chloride and catalytic amounts of DMF, and immediately added under anhydrous conditions to taxifolin in basic solution (Scheme 1) [6,16]. Extensive purification by column chromatography after the workup was necessary to remove all byproducts and obtain the pure compounds 7-*O*-cinnamoyltaxifolin **1** and 7-*O*-feruloyltaxifolin **2**.

2.1. Biological activity

2.1.1. Neuroprotection in HT22 cells

Oxytosis. Glutamate treatment of murine hippocampal HT22 cells leads to intracellular glutathione (GSH) depletion resulting in a form of programmed cell death due to oxidative stress [22]. This assay, also called oxidative glutamate toxicity, has a mechanistic association with aging and AD as GSH reduction is seen in the aging brain and is accelerated in AD [23]. Due to the generality of this toxicity pathway, oxytosis was used to investigate the ability of 7-*O*-cinnamoyltaxifolin **1** and 7-*O*-feruloyltaxifolin **2** to protect against oxidative stress in HT22 cells. As shown in Fig. 2A and C, **1** and **2** were highly protective against glutamate-induced oxidative stress, exceeding the beneficial effect of 25 μM quercetin, which served as a positive control. Compound **1** showed the highest neuroprotective activity at a concentration of 5 μM rescuing 74% of the cells (Fig. 2A). Taxifolin, cinnamic acid and the equimolar mixture of both were not neuroprotective at the tested concentrations of 1, 5 and 10 μM (Fig. 2A). The same neuroprotective pattern was observed for **2** and the respective controls taxifolin, ferulic acid and the one-to-one mixture of taxifolin and ferulic acid. None of the individual compounds nor the equimolar mixture showed any neuroprotective activity at the concentrations tested, but the ester hybrid **2** was highly protective at 5 μM with 70% cell viability compared to cells treated with glutamate only (Fig. 2C). The compounds were also investigated with regard to their toxicity in the absence of glutamate and both **1** and **2** were found to exhibit a slight, dose-dependent neurotoxic effect (Fig. 2B and D). However, for both **1** and **2**, greater than 70% of the cells survived even at the highest concentration tested (Fig. 2B and D).

Ferroptosis. Ferroptosis is a cell death pathway closely related if not identical to oxytosis [24]. Both forms of programmed cell death due to oxidative stress are consequences of GSH depletion, accumulation of reactive oxygen species (ROS) including lipid peroxides, mitochondrial dysfunction and a final influx of Ca^{2+} from the extracellular space [25]. Distinct from oxytosis which is induced by glutamate inhibiting cystine import by blocking system x_c^-, oxidative stress in the ferroptosis assay can be induced downstream in the cascade by inhibition of glutathione peroxidase 4 (GPx4). GPx4 is a GSH-dependent antioxidant enzyme which loses activity under GSH depletion, but can also be inhibited directly via covalent interaction of the compound RSL3 with the active site selenocysteine of GPx4 [26]. As shown in Fig. 3, both 7-*O*-esters of

taxifolin, **1** and **2**, were neuroprotective against ferroptosis whereas the individual components and the respective equimolar mixture did not exhibit any protective activity at the tested concentrations. At 5 μM, compound **1** rescued 80% of the cells and its effect remained at the higher concentration (Fig. 3A). The effect of compound **2** was weaker at 5 μM compared to compound **1** with around 40% cell survival (Fig. 3B), but at 10 μM both compounds were equally potent neuroprotectants, exceeding by far the effect of the controls.

ATP depletion. Energy metabolism and ATP levels in the brain decrease with age, as a consequence of a breakdown in neuronal energy production, and are associated with nerve cell damage and death in AD [27]. Iodoacetic acid (IAA), an irreversible inhibitor of the glycolytic enzyme glyceraldehyde 3-phosphate dehydrogenase, was used to induce ATP loss in HT22 cells [28]. 7-*O*-Cinnamoyltaxifolin **1** and 7-*O*-feruloyltaxifolin **2** were investigated towards their ability to protect against ATP loss and found to significantly increase cell survival in contrast to taxifolin, the respective phenolic acid and the mixture of both (Fig. 4). Compound **1** showed an effect already at 1 μM with 40% cell survival. The effect was lost at lower concentrations (data not shown). As observed in the assays described above, the esters **1** and **2** remarkably outshown the effects of the individual components and the one-to-one mixture of the flavonoid and the phenolic acid as potential hydrolysis products.

GSH quantification. As GSH and GSH-dependent enzymes provide the major line of defense in the protection towards oxidative stress in cells and GSH levels decrease with age [23], we were interested in whether the neuroprotective esters 7-*O*-cinnamoyltaxifolin **1** and 7-*O*-feruloyltaxifolin **2** had an influence on total glutathione levels (tGSH) in HT22 cells. Therefore, tGSH levels were determined in the presence of increasing concentrations of **1** and **2**. The equimolar mixture of taxifolin and the respective acid served as controls (Fig. 5). In cells treated only with the compounds, GSH levels were maintained by both compound **1** and the one-to-one mixture (Fig. 5A, black lines). Even though the GSH concentrations of **1**-treated cells were higher than the control starting from 2.5 μM and increased dose-dependently, the difference observed was not statistically significant. However, when HT22 cells were treated with 5 mM glutamate to induce oxytosis, tGSH levels were significantly increased by **1** whereas the presence of the equimolar mixture of taxifolin and cinnamic acid had no effect on the loss of tGSH seen in the presence of glutamate (Fig. 5A, blue lines). As shown in Fig. 5B, the one-to-one mixture of taxifolin and ferulic acid had no influence on tGSH in the absence of glutamate, while compound **2** increased tGSH levels even though the effect was not statistically significant (black lines). The decreased levels of tGSH in the presence of glutamate were significantly elevated by compound **2** at 10 μM where the equimolar mixture of taxifolin and ferulic acid had no effect (Fig. 5B, blue lines). Thus, compounds **1** and **2** both influence tGSH levels and increase tGSH under oxidative stress induced by glutamate treatment in HT22 cells although **1** shows a larger effect at lower concentrations than **2**.

2.1.2. Anti-inflammatory effects in BV-2 cells

NO and cytokines. Microglial cells are the resident immune cells of the CNS. Their activation to the pro-inflammatory phenotype
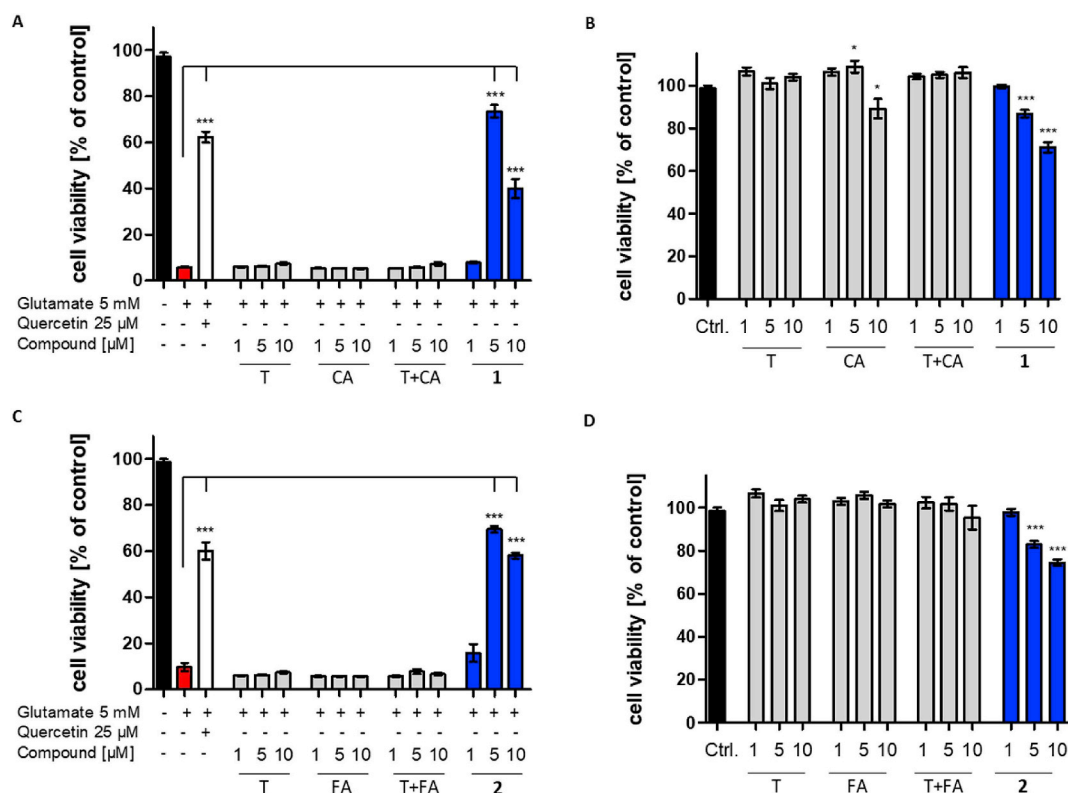
Fig. 2. Oxytosis assay in HT22 hippocampal nerve cells. 25 µM Quercetin served as a positive control (white) while 5 mM glutamate was used to induce toxicity (red). **A)** Neuroprotective effect of 7-*O*-cinnamoyltaxifolin (**1**) and the controls taxifolin (T), cinnamic acid (CA) and the equimolar mixture of taxifolin and cinnamic acid (T + CA). **B)** Neurotoxicity of the compounds taxifolin (T), cinnamic acid (CA), the one-to-one mixture (T + CA) and compound **1**. **C)** Neuroprotective effect of 7-*O*-feruloyltaxifolin (**2**) and the controls taxifolin (T), ferulic acid (FA) and the one-to-one mixture of taxifolin and ferulic acid (T + FA). **D)** Neurotoxic effect of the compounds taxifolin (T), ferulic acid (FA), the equimolar mixture (T + FA) and compound **2**. Data is presented as means ± SEM of three independent experiments and results refer to untreated control cells (black). Statistical analysis was rendered using One-way ANOVA followed by Dunnett's multiple comparison posttest using GraphPad Prism 5 referring to cells treated with 5 mM glutamate only in **A)** and **C)** or to untreated control cells in **B)** and **D)**. Levels of significance: *$p < 0.01$; ***$p < 0.001$. (For interpretation of the references to color in this figure legend, the reader is referred to the Web version of this article.)

contributes to neuroinflammation, a major hallmark of AD [29]. Uncontrolled activation of microglia can lead to production of various pro-inflammatory and cytotoxic factors, like cytokines, free radicals, excitatory neurotransmitters and eicosanoids contributing to neuronal injury and neurodegeneration [29]. Thus, inhibition of pro-inflammatory microglia activation is another important target in the context of AD. BV-2 mouse microglial cells were used to investigate the ability of **1** and **2** to counteract inflammation induced by bacterial lipopolysaccharide (LPS). We were first interested in the effect of the compounds on nitric oxide (NO) production as a pro-inflammatory mediator (Fig. 6A and B). Both 7-*O*-esters **1** and **2** strongly reduced NO production. The levels were decreased dose-dependently in an overadditive manner with a significant effect already at 2.5 µM. As with the neuroprotective effects in the HT22 cells, this again exceeded the effect of the individual components and the equimolar mixture, where only ferulic acid displayed weak activity at higher concentrations. At a concentration of 10 µM, 7-*O*-cinnamoyltaxifolin **1** decreased NO production to only 13% compared to cells treated only with LPS (Figure 6A) and 7-*O*-feruloyltaxifolin **2** decreased the production to 16% NO (Fig. 6B). Compound **1** was further examined towards its effect on the cytokines IL6 and TNFα (Fig. 6C) using ELISAs. At 10 µM, taxifolin, cinnamic acid, the one-to-one mixture and **1** reduced induction of TNFα to less than 40%. Even though the levels of TNFα were decreased strongest by **1**, the difference to the controls taxifolin and cinnamic acid as well as the one-to-one mixture of both was not statistically significant (Fig. 6C). A stronger difference was seen with IL6 induction which was significantly reduced by compound **1** compared to cinnamic acid and the equimolar mixture of taxifolin and cinnamic acid (Fig. 6C). As

compound **1** did not show an enhanced effect on TNFα levels as compared to the respective controls, compound **2** was only assessed for its effect on IL6 levels using an ELISA. Although IL6 levels were decreased by compound **2** (Fig. 6D), the difference from the controls was not statistically significant.

Nrf2 upregulation. Previously, taxifolin esterified in position 7 with gallic acid was shown to upregulate the nuclear factor (erythroid-derived 2)-like 2 (Nrf2) pathway in RAW264.7 cells [16], a macrophage cell line. Since brain microglial cells have many properties similar to peripheral macrophages and, of the two compounds, compound **1** was the strongest reducer of neuroinflammation markers in the BV-2 cells, we asked whether Nrf2 was involved in its mode of action. Nuclear fractions of BV-2 cells treated with the compounds were subjected to Western blot analysis. As shown in Fig. 7A, 7-*O*-cinnamoyltaxifolin **1** dose-dependently increased nuclear Nrf2 levels up to 24-fold at 10 µM after 4 h of incubation. Taxifolin and the equimolar mixture of taxifolin and cinnamic acid did not induce Nrf2 translocation to the nucleus. Next, we were interested in whether Nrf2 was directly involved in the anti-inflammatory effects of **1** and so downregulated Nrf2 in BV-2 microglia by transfection using specific siRNA. Fig. 7B shows the effective downregulation of Nrf2 in cells treated with siNrf2 (lane 3) even in the presence of the strong inducer **1** (lane 4), compared to the nonspecific control siRNA (lanes 1 and 2). The siRNA modified BV-2 cells were then used for the LPS inflammation assay. As shown in Fig. 7C, no shift in the dose-response curve for NO reduction was observed between Nrf2 knockdown cells and the control, therefore Nrf2 knockdown had no effect on the anti-inflammatory activity of **1**.

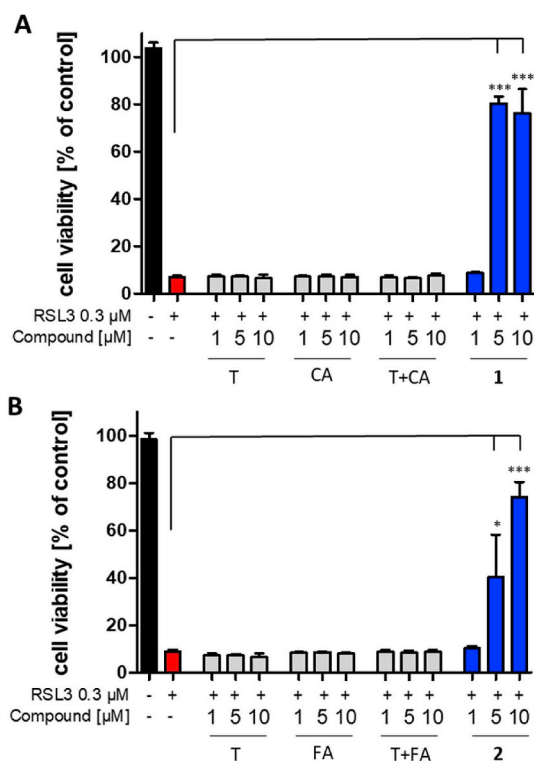**Cellular uptake experiments.** Semisynthetic gallic acid esters of

Fig. 3. Ferroptosis was induced in HT22 cells with 300 nM RSL3. **A)** Neuroprotective effect of 7-*O*-cinnamoyltaxifolin (**1**) and the controls taxifolin (T), cinnamic acid (CA) and the equimolar mixture of taxifolin and cinnamic acid (T + CA). **B)** Neuroprotective effect of 7-*O*-feruloyltaxifolin (**2**) and the controls taxifolin (T), ferulic acid (FA) and the one-to-one mixture of taxifolin and ferulic acid (T + FA). For both **A)** and **B)**, data is presented as means ± SEM of three independent experiments and results refer to untreated control cells (black). Statistical analysis was rendered using One-way ANOVA followed by Dunnett's multiple comparison posttest using GraphPad Prism 5 referring to cells treated with 300 nM RSL3 only (red). Levels of significance: *$p < 0.01$; ***$p < 0.001$. (For interpretation of the references to color in this figure legend, the reader is referred to the Web version of this article.)

Fig. 4. HT22 cells were treated with 20 µM iodoacetic acid (IAA) to induce ATP depletion in the absence or presence of the compounds. **A)** Protective effect of 7-*O*-cinnamoyltaxifolin (**1**) and the controls taxifolin (T), cinnamic acid (CA) and the equimolar mixture of taxifolin and cinnamic acid (T + CA). **B)** Protective effect of 7-*O*-feruloyltaxifolin (**2**) and the controls taxifolin (T), ferulic acid (FA) and the one-to-one mixture of taxifolin and ferulic acid (T + FA). For both **A)** and **B)**, data is presented as means ± SEM of three independent experiments and results refer to untreated control cells (black). Statistical analysis was rendered using One-way ANOVA followed by Dunnett's multiple comparison posttest using GraphPad Prism 5 referring to cells treated with 20 µM IAA only (red). Levels of significance: ***$p < 0.001$. (For interpretation of the references to color in this figure legend, the reader is referred to the Web version of this article.)

taxifolin have been shown to be converted to quercetin derivatives in RAW264.7 cells by Vrba et al. [16]. Therefore, we were interested if we could detect cellular uptake of our synthetic hybrid 7-*O*-cinnamoyltaxifolin **1** in murine BV-2 microglia cells, and if the compound was hydrolyzed or was converted to the respective 7-*O*-quercetin ester, as described before [16]. We first recorded a reference HPLC chromatogram with 50 ng of each compound to determine their retention times (Fig. 8A). For cellular uptake experiments, BV-2 cells were incubated with 50 µM 7-*O*-cinnamoyltaxifolin **1** for 0, 30, 90 and 240 min and lysates were analyzed by HPLC (Fig. 8B). Fig. 8B–a shows that already for time point 0, where cells were lysed immediately after the addition of the compound, next to the peak for **1** at 43.9 min, a second peak was detected with a retention time of 48.9 min. After 30 min both peaks increased in intensity (Fig. 8B–b) and a shift towards the second peak was observed after 90 min incubation (Fig. 8B-c), indicating that the compound was metabolized. After 4 h, compound **1** was only detected in trace amounts and also the second peak decreased (Fig. 8B–d). Both compounds were found to be stable towards their potential hydrolysis products as no additional peaks were detected at lower retention times that would correspond to the reference compounds in Fig. 8A. To ensure that conversion of 7-*O*-cinnamoyltaxifolin was indeed dependent on the presence of cells, 50 µM **1** were incubated for 30 min in culture medium only. HPLC analysis gave one distinct peak with a retention time of 44.0 min and no further compounds were detected (Fig. 8C). To confirm the identity of the detected compounds, the two peaks at 43.9
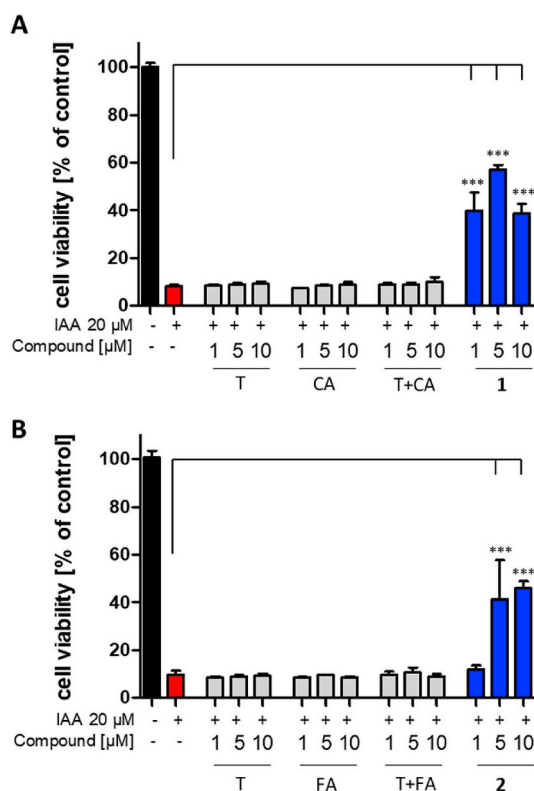
and 48.9 min were collected and submitted to MS analysis respectively. In Fig. 8D the peak with a retention time of 43.9 min was identified as 7-*O*-cinnamoyltaxifolin with $m/z = 435.11$ ([M+H]$^+$ calc. = 435.11). MS/MS fragmentation resulted in signals at $m/z = 305.07$ corresponding to taxifolin and at $m/z = 131.05$ and $m/z = 103.05$ corresponding to cinnamic acid (minus H_2O and additional loss of CO, respectively). MS analysis of peak 2 with a retention time of 48.9 min gave signals at $m/z = 433.09$ corresponding to 7-*O*-cinnamoylquercetin with a calculated [M+H]$^+$ $m/z = 433.09$ (Fig. 8E). The compound was confirmed by MS/MS fragmentation where the masses of cinnamic acid ($m/z = 131.05$ and $m/z = 103.05$) and quercetin ($m/z = 303.05$) were identified.

***In vivo* studies.** To extend the *in vitro* studies, the esters **1** and **2** were evaluated and compared to the one-to-one mixtures of the respective acids and taxifolin regarding their protective effects against Aβ$_{25-35}$-induced memory impairment in a mouse model of AD, which has been described in detail before [21,30,31]. AD-like cognitive dysfunction was induced by intracerebroventricular (icv) injection of oligomerized Aβ$_{25-35}$ peptide into the mouse brain on day 1. Compounds were injected intraperitoneally (ip) from day 1 to day 7, and spatial working memory was evaluated on day 8 in a Y-maze assay. On days 9 and 10 of the study, a step-through passive-avoidance assay was performed as a measure of long-term memory improvement, followed by
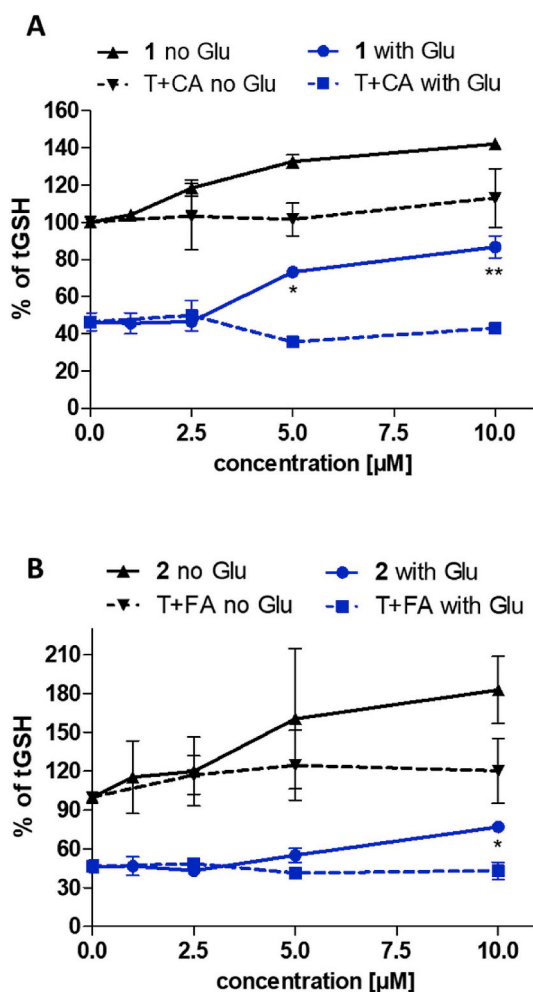
A

B

Fig. 5. Dose dependent effects of 7-*O*-cinnamoyltaxifolin **1** (**A**) and 7-*O*-feruloyltaxifolin **2** (**B**) and the equimolar mixtures (T + CA in **A** and T + FA in **B**) on total glutathione (tGSH) levels in HT22 cells in the absence (black lines) or presence (blue lines) of 5 mM glutamate (Glu) to induce oxytosis. GSH levels were measured in a chemical assay after 24 h and normalized to total protein. Results are given as mean ± SEM and were analyzed by One-way ANOVA followed by Dunnett's multiple comparison posttest using GraphPad Prism 5 referring to cells with no compound added. Levels of significance: *$p < 0.05$, **$p < 0.01$. (For interpretation of the references to color in this figure legend, the reader is referred to the Web version of this article.)

sacrifice on day 11. Solutions of compounds in 60% DMSO +40% saline (0.9%) were prepared directly before injection and injected ip once per day to achieve a dose of 1, 3, and 10 mg/kg, respectively. 60% DMSO +40% saline (0.9%) were used as vehicle (V) for control groups. The treatments did not affect the mouse body weight gain significantly during the week of therapy showing good tolerability (Fig. 11). Animals recovered quickly (within 10 min) from the icv injection stress after day 1.

Spatial working memory. Compound **2** reduced the Aβ_{25-35}–induced spontaneous alternation deficits at all doses tested (Fig. 9A). Compound **1** showed significant prevention of the Aβ_{25-35}-induced alternation deficit at 3 and 10 mg/kg (Fig. 9B). The esters **1** and **2** appeared to be significantly more neuroprotective than the mixtures of taxifolin and the respective acids (Fig. 9C,D,E).

Long-term memory. On day 9 of the study, the step-through passive-avoidance training was conducted, followed by the assessment of the step-through latency on day 10 as described earlier [21,30,31]. None of the compounds or mixtures improved the Aβ-induced impairment of long-term memory in prolongation of step-through (Fig. 10).

3. Discussion

In this work we present the synthesis and detailed *in vitro* and *in vivo* evaluation of two natural product hybrids, 7-*O*-cinnamoyltaxifolin **1** and 7-*O*-feruloyltaxifolin **2**, with overadditive neuroprotective effects. The compounds' design was based on interesting results of a SAR study for silibinin esters [6] and the beneficial pleiotropic effects of taxifolin and the phenolic acids as neuroprotectants [32,33] to address multifactorial neurodegenerative diseases like AD. For silibinin, the influence of the individual hydroxyl groups was investigated and position 7 was assigned with a rather pro-oxidant character [34] and therefore was protected by esterification with the antioxidant phenolic acid [6]. As the catechol moiety of the flavonoid taxifolin is a strong antioxidant group itself and modifications on the A-Ring are well tolerated, taxifolin was chemically connected via an ester bond in position 7 to the phenolic acids cinnamic and ferulic acid, which were the superior phenolic acids in the SARs of silibinin esters [6] and counteract pathways of neurodegeneration as described above.

Due to multiple hydroxyl groups, selective esterification of flavonoids is a challenging task and often requires the use of protective groups [35]. Vrba et al. synthesized taxifolin and quercetin esters with gallic acid by using benzyl-protected gallic acid, or benzyl-protected quercetin for esterification in position 3 of the flavonoid [16]. Protection and deprotection steps enlarge the synthetic route and might narrow the yield of target compounds. Similar to the conditions applied before for the synthesis of silibinin esters [6,36] we synthesized the 7-*O*-esters of taxifolin by direct acylation without the use of protective groups. Acyl chlorides of cinnamic or ferulic acid were prepared using oxalyl chloride and catalytic amounts of DMF in tetrahydrofuran (THF) and were added to a solution of taxifolin in THF basified with triethylamine. Optimized reaction conditions even allowed the generation of the feruloyl chloride *in situ* for esterification without protecting the free hydroxyl group.

As the single-target approach has not proven successful for the development of effective drugs against AD up to now, our approach was to characterize the compounds in a broad range of assays developed to reflect the biology of aging and neurodegeneration [37]. This approach is also an asset from a medicinal chemists point of view, as for molecules bearing a Michael system like cinnamic and ferulic acid, it is important to choose a variety of assays estimating the biological activity to avoid false-positive readouts (PAINS) [7]. Here, we used two different cell lines for the biological characterization. HT22 hippocampal nerve cells to study the neuroprotective effects of 7-*O*-cinnamoyltaxifolin **1** and 7-*O*-feruloyltaxifolin **2** against different types of oxidative stress, and mouse BV-2 microglia cells to examine the esters' anti-neuroinflammatory activity. In all cell-based assays, the compounds **1** and **2** showed strong and pronounced overadditive effects. The individual ester components taxifolin and the respective phenolic acids were not neuroprotective in any of our assays, neither was their equimolar mixture representing the potential hydrolysis products. In the rather low concentration range investigated, only the 7-*O*-esters were able to rescue cells from oxytosis, ferroptosis and ATP depletion in HT22 cells and LPS-induced neuroinflammation in BV-2 cells. These findings indicate a specific intracellular mode of action of 7-*O*-cinnamoyltaxifolin **1** and 7-*O*-feruloyltaxifolin **2** with the chemical connection contributing to the biological activity. Flavonoids have been shown to influence GSH levels as part of their antioxidant effect [38] and GSH is developing into an therapeutic objective for the treatment of oxidative stress-related diseases [39]. Compound **1** and **2**, but not the one-to-one mixture of taxifolin and the respective phenolic acid, were able to significantly increase GSH levels in HT22 cells under glutamate-induced oxidative stress.

Nrf2 is an important transcription factor that acts on the antioxidant response element (ARE) and has been shown to be induced by flavonoids [40]. As Nrf2 also has anti-inflammatory effects [41], we investigated the role of Nrf2 in the anti-inflammatory action of 7-*O*-
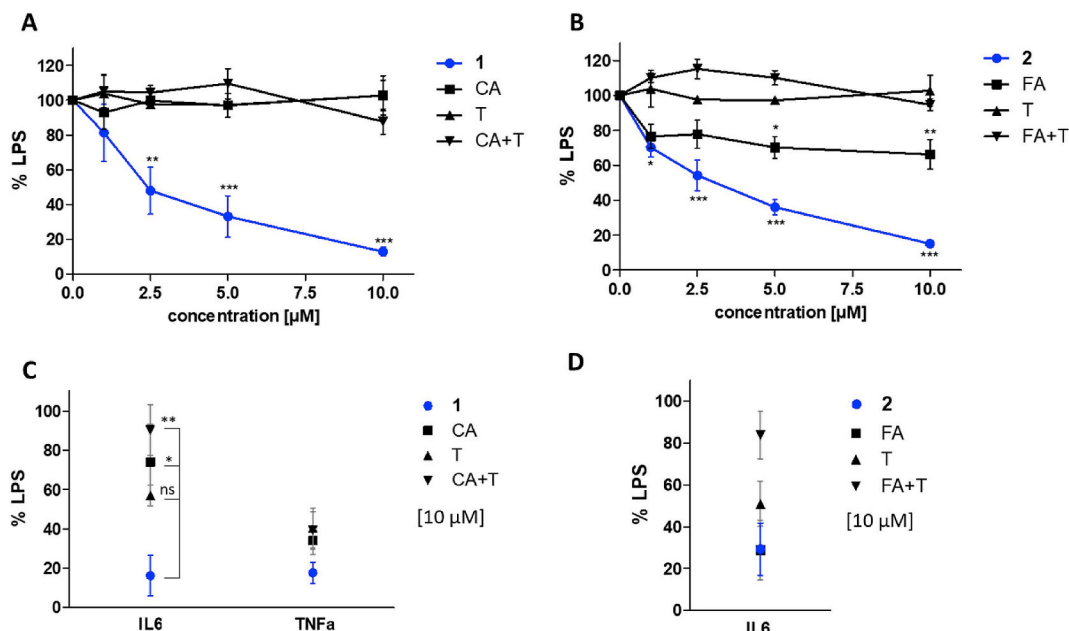
Fig. 6. Effects of **1** and **2** and the respective controls on the production of NO and pro-inflammatory cytokines IL6 and TNFα by LPS-treated BV-2 microglia cells. Cells were treated overnight with 50 ng/mL LPS alone or in the presence of 7-*O*-cinnamoyltaxifolin (**1**), cinnamic acid (CA), taxifolin (T) and the one-to-one mixture of both (T + CA) (**A** and **C**) or with 7-*O*-feruloyltaxifolin (**2**), ferulic acid (FA), taxifolin (T) and the equimolar mixture of the individual components (T + FA) (**B** and **D**). Supernatants were cleared and NO was quantified by the Griess assay. Data in in **A** and **B** are given as means ± SEM and relative to BV-2 cells treated with LPS only, which were set as 100%. One-way ANOVA was used for statistical analysis followed by Dunnett's multiple comparison posttest. Levels of significance: *$p < 0.05$, **$p < 0.01$, ***$p < 0.001$. **C**) The effect of 10 μM **1** on levels of the pro-inflammatory cytokines IL6 and TNFα after LPS-treatment was assessed using ELISAs as was the effect of 10 μM **2** on IL6 (**D**). For **C**) and **D**) Results are presented as percent (%) of the values obtained for treatment with LPS alone, which were set as 100% and are shown means ± SEM. Levels of significance: *$p < 0.05$, **$p < 0.01$ of One-way ANOVA followed by Tukey's posttest.
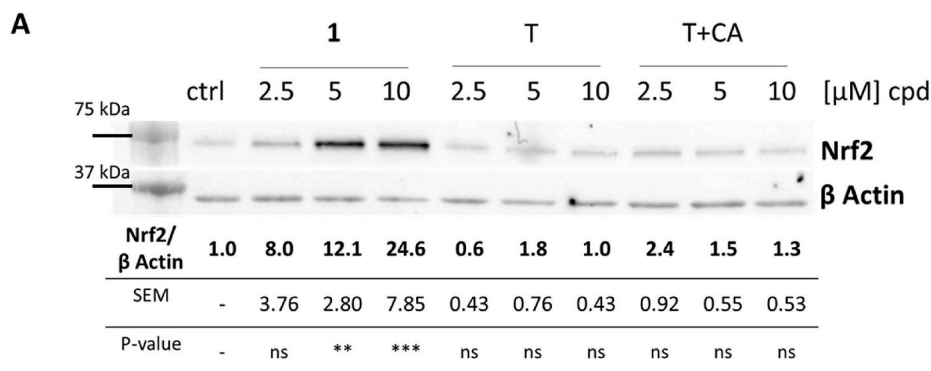

Fig. 7. Correlation of 7-*O*-cinnamoyltaxifolin **1** and Nrf2 in BV-2 microglia cells. **A)** Cells were treated for 4 h with DMSO as control or with increasing concentrations of **1**, taxifolin (T) or the equimolar mixture of taxifolin and cinnamic acid (T + CA). Nuclear fractions of BV-2 cells were prepared and analyzed by Western blot for Nrf2 using a specific antibody. Levels of Nrf2 were normalized to actin and a representative blot is shown. **B)** Transfection of BV-2 cells with control siRNA or Nrf2 siRNA. Nuclei of cells incubated with **1** or vehicle (DMSO control) for 4 h were analyzed by Western blots for Nrf2. **C)** Griess assay for NO quantification of transfected cells treated with increased concentrations of 7-*O*-cinnamoyltaxifolin **1**.
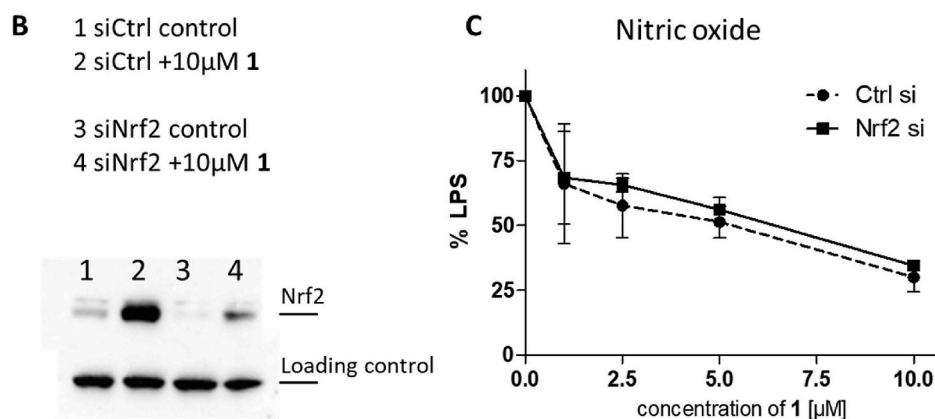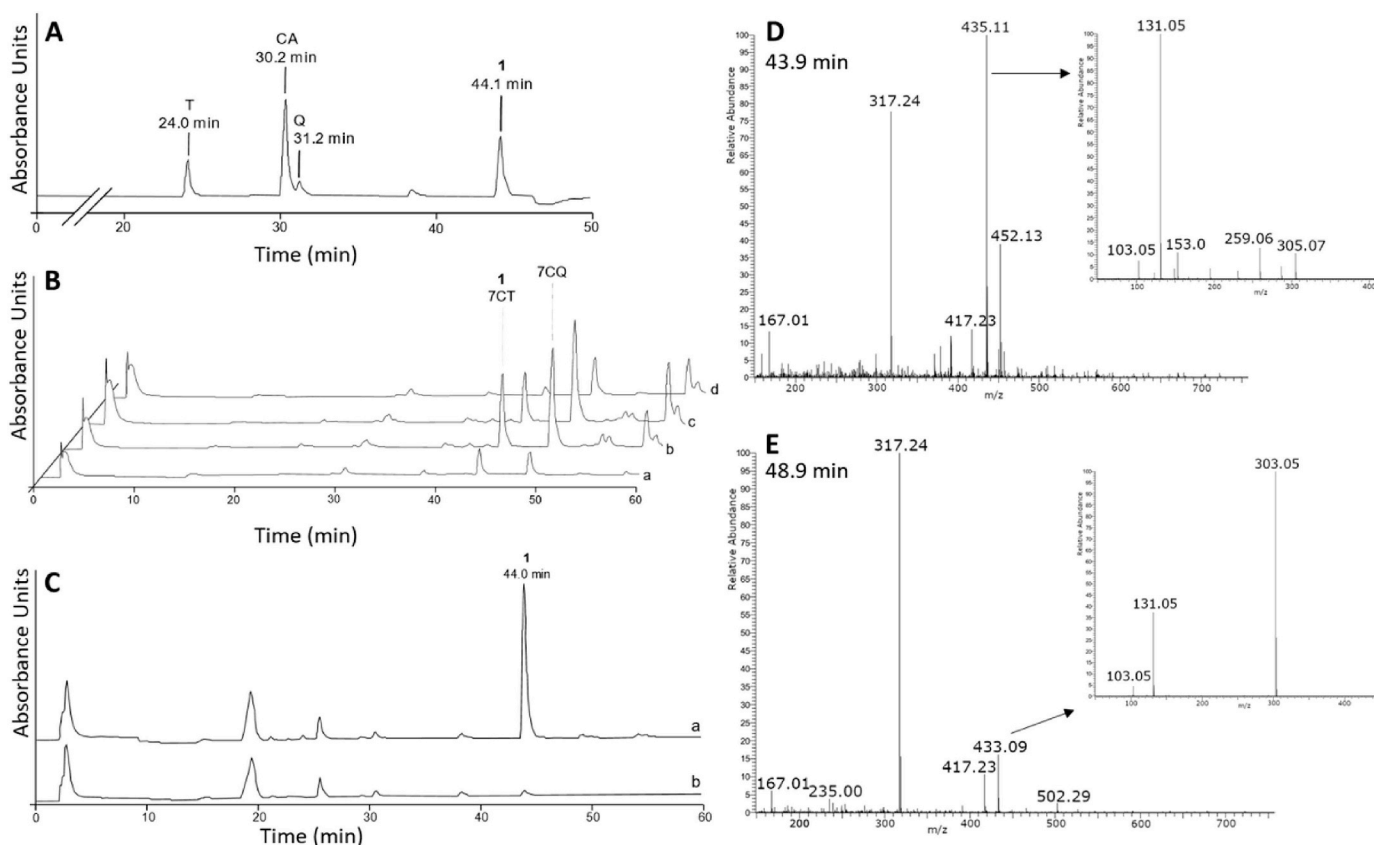
Fig. 8. Cellular uptake of compound **1**. **A)** 50 ng of taxifolin (T), cinnamic acid (CA), quercetin (Q) and 7-*O*-cinnamoyltaxifolin (**1**) were submitted to HPLC as reference for the compounds' retention times. **B)** 50 μM **1** were added to BV-2 cells and cells were immediately lysed (**a**), or incubated for 30 min (**b**), 90 min (**c**) or 4 h (**d**) prior to lysis and sample preparation. **C)** Incubation of 50 μM **1** for 30 min in medium only did not lead to compound conversion (**a**). (**b**): blank chromatogram with medium only. **D)** MS spectrum of the first HPLC peak (43.9 min) after incubating **1** for 30 min with BV-2 cells. The signal at $m/z = 435.11$ corresponds to **1** and was isolated for MS/MS fragmentation (inset) where $m/z = 131.05$ and $m/z = 305.07$ were detected corresponding to cinnamic acid and taxifolin, respectively. **E)** MS spectrum of the 48.9 min fraction gave a signal at $m/z = 433.09$ and the MS/MS fragmentation (inset) of the selected ion at $m/z = 131.05$ and $m/z = 303.05$ fit the m/z values of cinnamic acid and quercetin.

cinnamoyltaxifolin **1**. Compound **1** was a strong inducer of Nrf2 in BV-2 cells with more than a 20-fold increase in Nrf2 levels in the nuclear fraction, again in an overadditive manner. However, the anti-inflammatory effect of **1** was not dependent on Nrf2. BV-2 cells transfected with Nrf2 siRNA still showed reduced levels of NO as an inflammation marker upon treatment with **1** in a concentration dependent manner. Therefore, the exact pathways mediating the anti-inflammatory effects of **1** remain unclear and in future investigations

proteins of the NFKB pathway, like pIKBα, or MAP kinases could be considered [40].

The BV-2 cell line was also used for cellular uptake experiments to study the intracellular behavior of the compound. Instead of hydrolysis of the ester bond, we observed the conversion of 7-*O*-cinnamoyltaxifolin **1** to its oxidized quercetin derivative, in accordance to what Vrba et al. had shown for galloyl ester of taxifolin in RAW264.7 cells [16]. The oxidation product 7-*O*-cinnamoylquercetin was detectable right
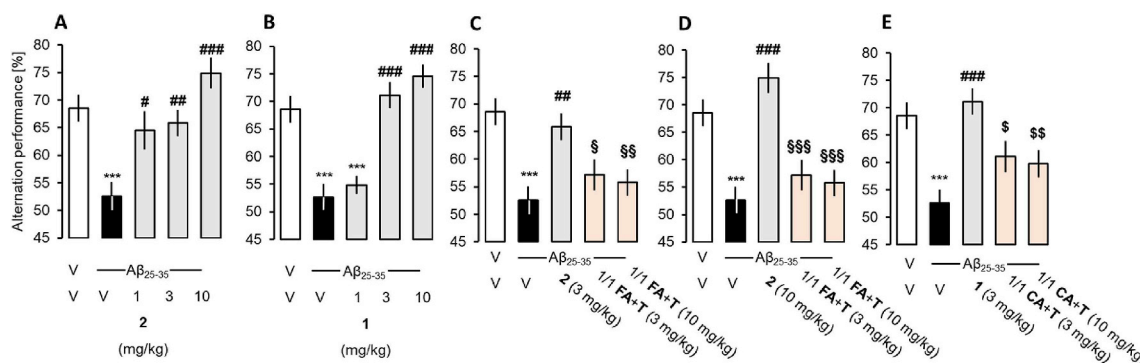

Fig. 9. Effect of the compounds on Aβ25-35-induced spontaneous alternation deficits in mice. V – vehicle, **2** – 7-*O*-feruloyltaxifolin, **1** – 7-*O*-cinnamoyltaxifolin, FA – ferulic acid, T – taxifolin, CA – cinnamic acid. Data shows mean ± SEM. ANOVA: $F_{(4,59)} = 8.77$, $p < 0.001$, $n = 11$–12 per group in **A)**; $F_{(4,58)} = 19.97$, $p < 0.001$, $n = 11$–12 in **B)**; $F_{(7,95)} = 7.35$, $p < 0.001$, $n = 11$–12 in **C)** and **D)**; $F_{(7,95)} = 8.54$, $p < 0.001$, $n = 11$–12 in **E)**. ***$p < 0.01$ vs. (V + V)-treated group; #$p < 0.05$, ##$p < 0.01$, ###$p < 0.001$ vs. (Aβ25-35 + V)-treated group; §$p < 0.05$, §§$p < 0.01$, §§§$p < 0.001$ vs. (Aβ25-35 + **2**)-treated group; $ $p < 0.05$, $$ $p < 0.01$ vs. (Aβ25-35 + **1**)-treated group; Dunnett's test.
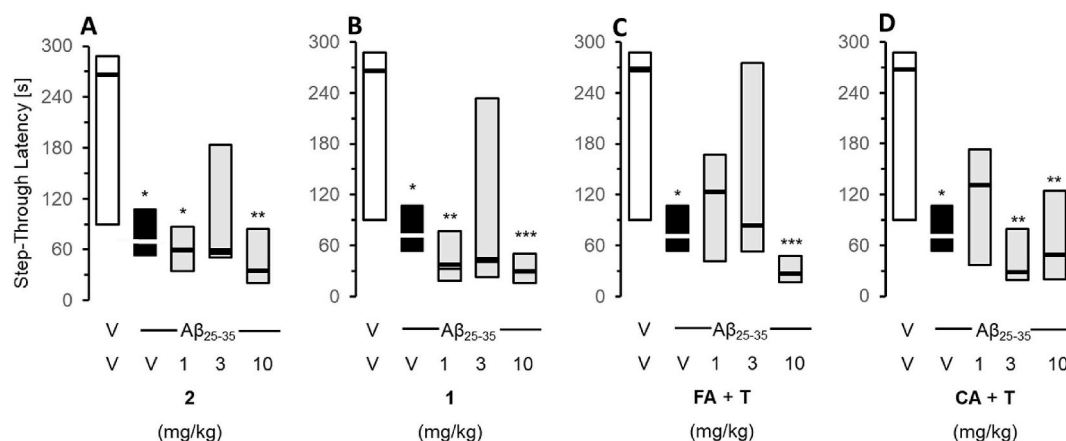
Fig. 10. Effect of the compounds on Aβ$_{25-35}$-induced passive avoidance impairments in mice. Data shows median and interquartile range. Kruskal-Wallis ANOVA: $H = 9.04$, $p < 0.1$, n = 12 per group in (**A**); $H = 15.0$, $p < 0.05$, n = 12 in (**B**); $H = 13.8$, $p < 0.05$, n = 12 in (**C**); $H = 12.0$, $p < 0.05$, n = 12 in (**D**). *$p < 0.05$, **$p < 0.01$, ***$p < 0.001$ vs. (V + V)-treated group; Dunn's test.

after addition of **1**, thus the intracellular oxidation occurred rapidly after cellular uptake and we were unable to determine which derivative contributes to what extent to the biological activity. However, the presence of cells was necessary for the conversion of the compound, as incubation of **1** in medium alone did not produce any metabolic by-product. Remarkably, even after 4 h incubation, none of the potential hydrolysis products expected were detected, proving the stability of the ester bond.

In vivo experiments with both compounds 7-*O*-cinnamoyltaxifolin **1** and 7-*O*-feruloyltaxifolin **2** showed their pharmacological relevance in an Aβ$_{25-35}$-induced memory impaired AD mouse model. The 7-*O*-esters of taxifolin, **1** and **2**, both showed significant improvement of spatial working memory in the Y-maze assay, although only moderate effects were seen in the non-spatial long-term memory passive avoidance test. A dichotomy between the resulting effects on Aβ$_{25-35}$-induced short-term and long-term memory deficits could however be predicted. Although silibinin ameliorated Aβ$_{25-35}$-induced memory deficits and oxidative stress, notably by mobilizing nitric-oxide synthase and TNFα [42,43], antioxidants including idebenone and α-tocopherol prevented the short-term memory deficits in the Y-maze and water-maze, but not passive avoidance deficits in Aβ$_{1-42}$-treated mice [44]. Another point is that taxifolin has a positive effect on Aβ$_{1-42}$ accumulation and aggregation [45,46]. We previously reported that a γ-secretase inhibitor, BMS-299897, attenuated Aβ$_{25-35}$-induced Aβ$_{1-42}$ seeding and toxicity [47]. Importantly, BMS-299897 blocked the Aβ$_{25-35}$-induced deficits in spontaneous alternation or novel object recognition, using a 1 h inter-trial time interval, but failed to affect the passive avoidance impairments or novel object recognition, using a 24 h intertrial time interval. Aβ$_{25-35}$ injection therefore provoked an accumulation in endogenous Aβ$_{1-42}$, an effect that was blocked by γ-secretase inhibition. This Aβ$_{1-42}$ accumulation marginally contributed to the toxicity or long-term memory deficits but likely plays a major role in synaptic dysfunction and short-term memory deficits. Thus, through this mechanism, taxifolin, and the related compounds **1** and **2**, may be particularly effective in alleviating these changes.

The effect of both 7-*O*-cinnamoyltaxifolin **1** and 7-*O*-feruloyltaxifolin **2** on short-term memory was remarkably superior to the effect evoked by the mixtures of taxifolin and the acids. Thereby, much greater effects on oxidative stress and protection from ATP depletion in the HT22 cells and the anti-neuroinflammatory effect in the BV-2 cells *in vitro* translates into an improved memory rescue *in vivo*, when neuroinflammation and neurotoxicity were induced by Aβ$_{25-35}$. Of note, both compounds **1** and **2** outperformed the symptomatic memory improvement of taxifolin which had been shown before [45,48]. These findings provide strong support for the general concept of 7-*O*-

esterification to improve the neuroprotective effects of taxifolin and show that this might also apply to other natural products with polyphenolic structures.

4. Conclusion

We showed that 7-*O*-esters of taxifolin and ferulic or cinnamic acid have pronounced neuroprotective effects against oxidative stress and neuroinflammation in a variety of assays in HT22 and BV-2 cell models, proving a pleiotropic beneficial effect which is desperately needed in the context of multifactorial neurodegenerative diseases like AD. Since the effects of 7-*O*-cinnamoyltaxifolin and 7-*O*-feruloyltaxifolin were overadditive in each of the assays used, one can conclude a specific cellular interaction distinct from the hybrids' building blocks. Due to the significant and overadditive *in vivo* effects in the Aβ$_{25-35}$-induced memory impaired AD mouse model, it can be assumed that the compounds were able to cross the blood-brain barrier and their metabolic stability was sufficient to evoke an amelioration of short-term memory defects in mice, in contrast to the controls. Even though their detailed mechanisms of action remains to be determined, several target pathways were identified including maintenance of GSH under conditions of stress and Nrf2 signaling. Thus, the natural product hybrids should be considered as a class of neuroprotective compounds with a distinct and specific pharmacological profile. This might also be true for other polyphenolic hybrids in addition to taxifolin-based esters. Future research aims to further develop the compounds as a potential starting point for drug development to treat neurodegenerative diseases, as their origin as dietary natural products provides medical value due to reduced toxicity and side effects with a pleiotropic pharmacological effect.

5. Experimental section

5.1. Chemical synthesis

General information. All reagents were used without further purification and bought from common commercial suppliers. For anhydrous reaction conditions, THF was dried prior to use by refluxing over sodium slices for at least 2 days under an argon atmosphere. Thin-layer chromatography was performed on silica gel 60 (alumina foils with fluorescent indicator 254 nm). UV light (254 and 366 nm) was used for detection. For column chromatography, silica gel 60 (particle size 0.040–0.063 mm) was used. Nuclear magnetic resonance (NMR) spectra were recorded with a Bruker AV-400 NMR instrument (Bruker, Karlsruhe, Germany) in DMSO-d6, and chemical shifts are expressed in

ppm relative to DMSO-d6 (2.50 ppm for 1H and 39.5 ppm for 13C). Purity of the synthesis products was determined by HPLC (Shimadzu Products), containing a DGU-20A3R degassing unit, a LC20AB liquid chromatograph, and an SPD-20A UV/vis detector. UV detection was measured at 254 nm. Mass spectra were obtained by a LCMS 2020 (Shimadzu Products). As a stationary phase, a Synergi 4U fusion-RP (150 mm × 4.6 mm) column was used, and as a mobile phase, a gradient of methanol/water with 0.1% formic acid. Parameters: A = water, B = methanol, V(B)/(V(A)+ V(B)) = from 5% to 90% over 10 min, V(B)/(V(A)+V(B)) = 90% for 5 min, V(B)/(V(A) + V (B)) = from 90% to 5% over 3 min. The method was performed with a flow rate of 1.0 mL/min. Compounds were only used for biological evaluation if the purity was ≥95%. Melting points were determined using an OptiMelt automated melting point system (Scientific Instruments GmbH, Gilching, Germany).

5.2. General procedure for the synthesis of 7-O-ester of taxifolin

The respective phenolic acid (1.5 equiv.) was dissolved in dry THF. 3 μL DMF and oxalyl chloride (1.5 equiv.) were added and the solution stirred at room temperature until TLC indicated complete conversion of the acid. Taxifolin (1.0 equiv.) was dissolved in dry THF and NEt$_3$ (2.0 equiv.) was added. The freshly prepared acid chloride was added dropwise to the taxifolin solution and the mixture stirred at room temperature for 2 h. The reaction was quenched by the addition of water and extracted with ethyl acetate. The organic layer was washed with 1 M HCl, brine and dried over NaSO$_4$ when the solvent was evaporated. The product was purified twice by column chromatography using 1.5%–3% methanol in CH$_2$Cl$_2$ with 1% formic acid.

7-O-Cinnamoyltaxifolin ((2R,3R)-2-(3,4-dihydroxyphenyl)-3,5-dihydroxy-4-oxochroman-7-yl cinnamate) **1**: Cinnamic acid (146 mg, 0.98 mmol, 1.5 equiv.) was dissolved in 5 mL dry THF. 3 μL DMF and oxalyl chloride (87.4 μL, 1.02 mmol, 1.5 equiv.) were added and stirred for 30 min when conversion of cinnamic acid into the acid chloride was complete. Taxifolin (200 mg, 657 μmol, 1.0 equiv.) was dissolved in 15 mL dry THF and NEt$_3$ (182.2 μl, 1.31 mmol, 2.0 equiv.) was added. Following the general procedure, compound **1** was purified twice by column chromatography to obtain the product as an off-white solid (125 mg, 0.28 mmol, 43%).

1H NMR (400 MHz, DMSO-d$_6$) δ = 11.73 (s, 1H), 9.01 (s, 2H), 7.86 (d, *J* = 16.0, 1H), 7.80 (dd, *J* = 7.2, 2.3, 2H), 7.47 (d, *J* = 1.7, 3H), 6.92 (d, *J* = 1.8, 1H), 6.86 (d, *J* = 16.0, 1H), 6.81–6.73 (m, 2H), 6.45 (d, *J* = 2.1, 1H), 6.42 (d, *J* = 2.1, 1H), 5.96–5.85 (m, 1H), 5.15 (d, *J* = 11.5, 1H), 4.69 (dd, *J* = 11.5, 5.6, 1H) ppm; **13C NMR** (101 MHz, DMSO-d$_6$) δ = 199.6, 164.0, 162.0, 161.9, 158.0, 147.2, 145.9, 145.0, 133.7, 131.1, 129.0 (2C), 128.8 (2C), 127.6, 119.5, 116.7, 115.5, 115.1, 104.8, 102.8, 101.7, 83.3, 71.9 ppm.

ESI: *m/z* calculated for C$_{24}$H$_{18}$O$_8$ [M+H]$^+$ 435.10, found: 435.15; HPLC purity: 98% (retention time: 12.7 min); mp: 189 °C.

7-O-Feruloyltaxifolin ((2R,3R)-2-(3,4-dihydroxyphenyl)-3,5-dihydroxy-4-oxochroman-7-yl (E)-3-(4-hydroxy-3-methoxyphenyl)acrylate) **2**: Ferulic acid (268 mg, 1.38 mmol, 1.1 equiv.) was dissolved in dry THF, 3 μL DMF and oxalyl chloride (224 μL, 2.62 mmol, 2.0 equiv.) were added and stirred until the acid chloride formation was complete. Taxifolin (400 mg, 1.31 mmol, 1.0 equiv.) was dissolved in dry THF and NEt$_3$ (726 μL, 5.24 mmol, 4.5 equiv.) was added. Following the general procedure, compound **2** was obtained as light-yellow foam (168 mg, 0.35 mmol, 27%).

1H NMR (400 MHz, DMSO) δ = 11.72 (s, 1H), 9.74 (s, 1H), 9.01 (m, 2H), 7.77 (d, *J* = 15.9 Hz, 1H), 7.42 (d, *J* = 1.9 Hz, 1H), 7.22 (dd, *J* = 1.9 Hz and 8.3 Hz, 1H), 6.91 (d, *J* = 1.9 Hz, 1H), 6.83 (d, *J* = 8.1 Hz, 1H), 6.78 (d, *J* = 1.9 Hz, 1H), 6.76 (d, *J* = 8.0 Hz, 1H), 6.70 (d, *J* = 15.9 Hz, 1H), 6.42 (d, *J* = 2.1 Hz, 1H), 6.38 (d, *J* = 2.1 Hz, 1H), 5.87 (d, *J* = 6.2 Hz, 1H), 5.13 (d, *J* = 11.5 Hz, 1H), 4.68 (dd, *J* = 6.1 Hz and *J* = 11.5 Hz, 1H), 3.83 (s, 3H) ppm. **13C NMR** (101 MHz, DMSO) δ = 199.6, 164.3, 162.0, 161.9, 158.2, 150.0, 148.0,

147.9, 145.9, 145.0, 127.6, 125.3, 123.9, 119.5, 115.6, 115.4, 115.1, 112.8, 111.5, 104.7, 102.8, 101.6, 83.3, 71.9, 55.7 ppm.

ESI: *m/z* calculated for C$_{25}$H$_{20}$O$_{10}$ [M+H]$^+$ 481.11; found 481.15; HPLC purity: 96% (retention time: 11.7 min); mp: 191 °C.

5.3. Cell culture general procedures

HT22 cells were grown in Dulbecco's Modified Eagle Medium (DMEM, Sigma Aldrich, Munich Germany) supplemented with 10% (v/v) fetal calf serum (FCS) and 1% (v/v) penicillin-streptomycin. BV-2 cells were grown in low glucose DMEM (Invitrogen, Carlsbad, CA, USA) supplemented with 10% FCS and 1% (v/v) penicillin-streptomycin. Cells were subcultured every two days and incubated at 37°C with 10% CO$_2$ in a humidified incubator.

Compounds were dissolved in dimethyl sulfoxide (DMSO, Sigma Aldrich, Munich, Germany) as stock solutions and diluted further into 1x phosphate-buffered saline (PBS).

For determination of cell viability, a colorimetric 3-(4,5-dimethylthiazol-2-yl)-2,5- diphenyl tetrazolium bromide (MTT, Sigma Aldrich, Munich, Germany) assay was used. MTT solution (5 mg/mL in PBS) was diluted 1:10 with medium and added to the wells after removal of the old medium. Cells were incubated for 3 h and then lysis buffer (10% SDS) was applied. The next day, absorbance at 560 nm was determined with a multiwell plate photometer (Tecan, SpectraMax 250).

Neurotoxicity and oxytosis in HT22 cells. 5×10^3 cells per well were seeded into sterile 96-well plates and incubated overnight. For the neurotoxicity assay, medium was removed and 1, 5, 10 or 25 μM of the compound diluted with medium from a 0.1 M stock solution was added to the wells. 0.05% DMSO in DMEM served as a control. Cells were incubated for 24 h when neurotoxicity was determined using a colorimetric MTT assay.

For the oxytosis assay, 5 mM glutamate (monosodium-L-glutamate, Sigma Aldrich, Munich, Germany) together with 1, 5 or 10 μM of the respective compound were added to the cells and incubated for 24 h. 25 μM quercetin (Sigma Aldrich, Munich, Germany) together with 5 mM glutamate served as a positive control. After 24 h incubation, cell viability was determined using a colorimetric MTT assay as described above. Results are presented as percentage of untreated control cells. Data is expressed as means ± SEM of three independent experiments. Analysis was accomplished using GraphPad Prism 5 Software applying Oneway ANOVA followed by Dunnett's multiple comparison posttest. Levels of significance: *p < 0.05; **p < 0.01; ***p < 0.001.

Ferroptosis in HT22 cells. 3×10^3 cells per well were seeded into sterile 96-well plates and incubated overnight. The next day medium was exchanged with fresh medium and 300 nM RSL3 was added with vehicle (DMSO) to induce oxidative stress, or together with 1, 5 or 10 μM of the respective compound for protection. After 24 h cell viability was determined using a colorimetric MTT assay. Results are presented as percentage of untreated control cells. Data are expressed as means ± SEM of three independent experiments. Analysis was accomplished using GraphPad Prism 5 Software applying Oneway ANOVA followed by Dunnett's multiple comparison posttest. Levels of significance: *p < 0.05; **p < 0.01; ***p < 0.001.

ATP depletion in HT22 cells. 3×10^3 cells per well were seeded into sterile 96-well plates and incubated overnight. The next day medium was exchanged with fresh medium. 20 μM iodoacetic acid (IAA) was added with vehicle (DMSO) as negative control, or together with 1, 5 or 10 μM of the respective compound for protection. After 2 h incubation at 37°C in the incubator, medium was aspirated, and fresh medium was applied and only the compounds at the same respective concentrations were added without IAA. After 24 h cell viability was determined using a colorimetric MTT assay. Results are presented as percentage of untreated control cells. Data are expressed as means ± SEM of three independent experiments. Analysis was accomplished using GraphPad Prism 5 Software applying Oneway

ANOVA followed by Dunnett's multiple comparison posttest. Levels of significance: $*p < 0.05$; $**p < 0.01$; $***p < 0.001$.

GSH quantification in HT22 cells. 3×10^5 cells per plate were seeded in sterile 60 mm cell culture dishes. After 24 h incubation medium was exchanged with fresh medium and the respective concentrations of compounds in the presence or absence of 5 mM glutamate were added. After 24 h incubation cells were scraped into ice-cold PBS and 10% sulfosalicylic acid was added at a final concentration of 3.3%. tGSH was measured by a recycling assay based on the reduction of 5,5-dithiobis(2-nitrobenzoic acid) with glutathione reductase and NADPH [49]. Results were normalized to protein recovered from the acid-precipitated pellet by treatment with 0.2 N NaOH at 37°C overnight. Protein levels were determined by the bicinchoninic acid assay (Pierce, Rockford, IL, USA).

Anti-inflammatory activity in BV-2 cells. 5×10^5 cells per plate were seeded in sterile 35 mm cell culture dishes. After overnight incubation medium was exchanged with fresh medium. The cells were pretreated with the respective compounds at the indicated concentrations for 30 min when 50 μg/mL bacterial lipopolysaccharide (LPS) was added. After 24 h incubation, the medium was collected, spun briefly to remove floating cells and 100 μL of the supernatant were assayed for nitrite using 100 μL of the Griess Reagent in a 96 well plate. After incubation for 10 min at room temperature the absorbance at 550 nm was read on a microplate reader. The levels of IL6 and TNFα in the supernatants were determined using ELISAs (R&D Systems, Minneapolis, MN, USA) according to the manufacturer's instruction. Results are normalized to cell number as assessed by the MTT assay as described above.

5.4. Western blots

Sample preparation. 3×10^5 BV-2 cells per 60 mm dish were grown for 24 h before treatment with the respective compounds at the indicated concentrations were. After 4 h incubation nuclear fractions were prepared. Cells were rinsed twice in ice-cold Tris-buffered saline (TBS), scraped into ice-cold nuclear fractionation buffer (10 mM HEPES pH 7.9, 10 mM KCl, 0.1 mM EDTA, 0.1 mM EGTA, 1 mM DTT, 1 mM Na_3VO_4, 1x protease inhibitor cocktail and 1 x phosphatase inhibitor cocktail) and incubated on ice for 15 min. NP40 at a final concentration of 0.6% was added, cells were vortexed and the nuclei were pelleted by centrifugation. Nuclear proteins were extracted by sonication of the nuclear pellet in nuclear fractionation buffer and the extracts were cleared by additional centrifugation. Protein concentrations were quantified by the bicinchoninic acid assay (Pierce, Rockford, IL, USA) and adjusted to equal concentrations. 5x Western blot sample buffer (74 mM Tris-HCl pH 8.0, 6.25% SDS, 10% β-mercaptoethanol, 20% glycerol) was added to a final concentration of 2.5x and samples were boiled for 5 min.

Western blotting. Equal amounts of protein (10–20 μg) per lane were used for SDS-PAGE. All samples were separated using 4–12% Criterion XT Precast Bis-Tris Gels (Biorad, Herculs, CA, USA). Proteins were transferred to nitrocellulose membranes and the quality of protein measurement, electrophoresis and transfer were checked by Ponceau S staining. Membranes were blocked with 5% skim milk in TBS-T (20 mM Tris buffer pH 7.5, 0.5 M NaCl, 0.1% Tween 20) for 1 h at room temperature and incubated overnight at 4 °C with the primary antibody diluted in 5% BSA in TBS/0.05% Tween 20. HRP-conjugated rabbit anti-actin (#5125, 1/20 000) from Cell Signaling (Danvers, MA, USA) and rabbit anti-Nrf2 (#sc-13032, 1/500) were used as primary antibody. Subsequently, blots were washed in TBS/0.05% Tween 20 and incubated for 1 h at room temperature in horseradish peroxidase goat ant-rabbit (Biorad) diluted 1/5000 in 5% skim milk in TBS-T. After additional washing, protein bands were detected by chemiluminescence using the ChemiDoc™ MP Imaging System (Biorad).

Transfection. BV-2 cells were plated with 5×10^5 cells per dish in 60 mm tissue culture dishes and 166 pmol Nrf2 siRNA (#sc-37049) or control siRNA (#sc-37007) (Santa Cruz Biotechnology) were used along

with RNAi max (Invitrogen) according to the manufacturer's instructions.

Cellular uptake experiments. 5×10^5 BV-2 cells were grown in 35 mm dishes overnight and then 50 μM **1** was added. Cells were incubated for the indicated time periods after which they were scraped and transferred to Eppendorf tubes. Samples were centrifuged, washed twice with ice-cold PBS and resuspended in 200 μL methanol with 5% acetic acid (v/v). After sonication, cell debris was pelleted by centrifugation and the supernatant was collected for HPLC and MS analysis. The reaction mixture was fractionated by reversed-phase HPLC employing a linear gradient (0–80% acetonitrile in 0.1% trifluoroacetic acid within 40–60 min). A Vydac C-18 column was used (1.2×150 mm) and absorbance was monitored at a wavelength of 330 nm.

Mass Spectrometry was performed using a ThermoFisher Q Exactive Hybrid Quadrupole Orbitrap mass spectrometer. Samples were introduced by direct electrospray infusion of the HPLC fractions diluted with a one-to-one mixture of methanol and water containing 0.1% formic acid. Full MS scans were recorded for the 150–750 m/z range. MS/MS fragmentation was performed on the major peaks which did not correspond with background signals. Fragmentation was achieved by higher-energy collisional dissociation (HCD) at normalized collision energy settings between 10 and 30%.

5.5. In vivo experiments

Protocols for the behavioral experiments were established and described previously [21,30,31,50]. The compounds **1**, **2**, and the mixtures of taxifolin and ferulic or cinnamic acid were tested for their neuroprotective properties against the toxicity of intracerebroventricular (icv) injection of the oligomerized Aβ$_{25-35}$ peptide in an *in vivo* pharmacological mouse model of AD [21]. All compounds were dissolved in 60% DMSO in saline (0.9%) and injected intraperitoneally (ip) once per day on days 1–7 of the study. The oligomerized Aβ$_{25-35}$ peptide was injected icv on the first day of the study. Behavioral evaluation of memory was performed between day 8 and 10, followed by sacrifice on day 11. Brain samples were collected and stored at −80°C awaiting further biochemical analysis.

Animals. For *in vivo* experiments, male Swiss mice (6 weeks old, weighing 31–36 g, from JANVIER (Saint Berthevin, France)) were used. Housing and experiments were conducted in the animal facility building of the University of Montpellier (CECEMA, Office of Veterinary Services agreement # B-34-172-23). Animals were randomly assigned to the different treatment groups and housed with access to food and water *ad libitum*, except during behavioral experiments. Temperature and humidity were controlled in the animal facility providing a 12 h/12 h light/dark cycle (lights off at 07:00 p.m.). All animal procedures were conducted in strict adherence to the European Union directive of September 22, 2010 (2010/63/UE) and the ARRIVE guidelines. The project was authorized by the French National Ethic Committee (APAFIS #1485–15034).

Preparation of compounds for injection. Compounds were weighed every day directly before injection, and dissolved in pure DMSO at a concentration of 3.33 mg/mL. The obtained stock solutions were diluted with saline (0.9%) to the test concentration with a final percentage of DMSO in saline of 60% for all compounds. 60% DMSO in saline was used as vehicle. Behavior of the mice in the home cages was checked visually after all injections, including the control of weight gain. As shown in Fig. 11, weight gain was not altered significantly indicating good compound and vehicle solution tolerability. Animals were tested in behavioral tests 24 h after the last compound/vehicle administration.

Amyloid peptides preparation and icv injection. Methods were described previously [21,30,50]. Briefly, mice were anesthetized with isoflurane 2.5% and Aβ$_{25-35}$ peptide (9 nmol in 3 μL/mouse) was injected icv. Aβ$_{25-35}$ peptide was prepared and injected according to
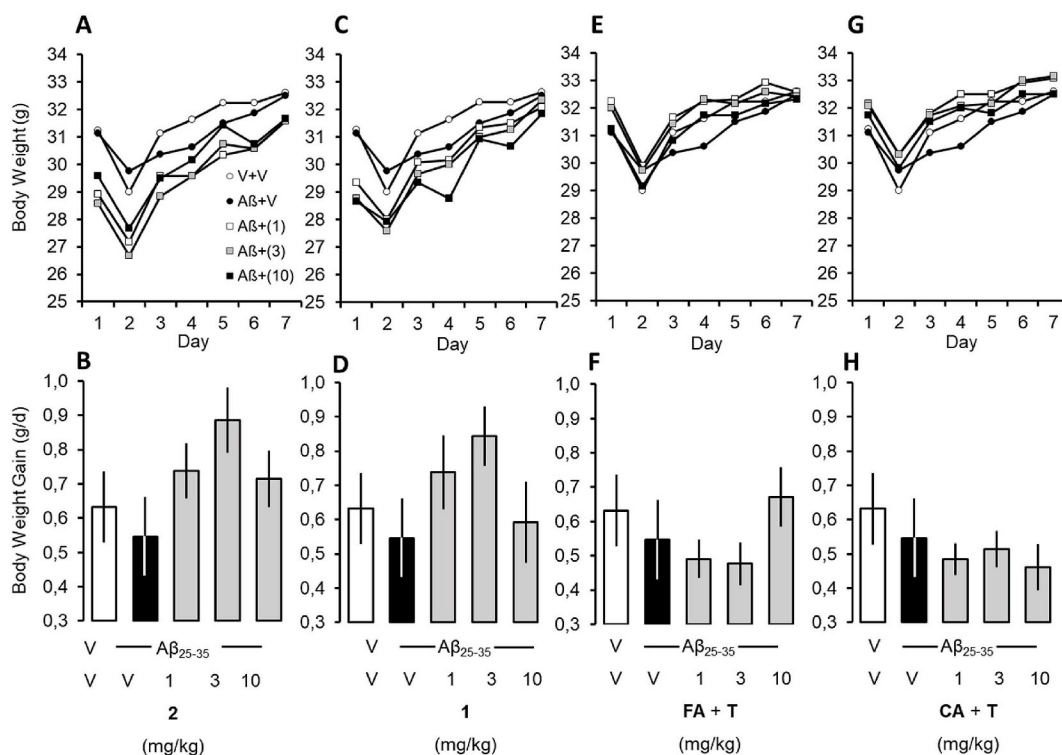
Fig. 11. Upper panel: development of the body weight; lower panel: average of weight gain from day 2–7. Data show mean (upper panel) or mean $\pm$ SEM (lower panel). Icv injection provoked a stress-induced acute weight loss, but animals recovered during the following days. ANOVA: $F_{(4,51)} = 1.73$, $p > 0.05$, n = 12 in (**B**); $F_{(4,51)} = 1.25$, $p > 0.05$, n = 12 in (**D**); $F_{(4,51)} = 1.20$, $p > 0.05$, n = 12 in (**F**); $F_{(4,51)} = 0.73$, $p > 0.05$, n = 12 in (**H**).

Maurice et al. [21] Icv injections of bidistilled water served as vehicle.

Spontaneous alternation performances in Y-maze. On day 8, spatial working memory of all mice was evaluated in the Y-maze [21,30,50]. The Y-maze consists of grey polyvinylchloride and 3 arms (40 cm long, 13 cm high, 3 cm wide at the bottom, 10 cm wide at the top, and converging at an equal angle). Every mouse is placed at the end of one arm and allowed to explore the maze freely for 8 min on its own. All entries into an arm (including returns into the same arm) were counted. From this, the number of arm entries and spontaneous alternations (mouse enters all three arms on consecutive occasion) were calculated (alternations/(arm entries-2) x 100).

Passive avoidance test. A passive avoidance test was performed on days 9 (training) and 10 (measurement of retention) to evaluate non-spatial long-term memory, as described previously [21,30,50]. For the experiment, a two-compartment (15 × 20 × 15 cm high) poly-vinylchloride box was used. Thereby, one compartment is white and illuminated with a bulb (60 W, 40 cm above the apparatus) and the other compartment is black with a cover and grid floor. The compartments are separated by a guillotine door. During the training session (day 9), every animal was placed in the white compartment and left to explore for 5 s. Then, the door was opened, and the mouse was able to explore into the dark compartment. After it entered the dark with all its paws touching the grid floor, the door was closed, and a foot shock was delivered (0.3 mA) for 3 s using a scrambled shock generator (Lafayette Instruments, Lafayette, USA). The time to enter the dark compartment (step-through latency), and the level of sensitivity to the shock evaluated (no sign = 0, flinching reactions = 1, vocalizations = 2) were recorded. The treatments did not affect the step-through latency or shock sensitivity in the present study (data not shown). On day 10, the mice were placed in the white compartment again and the door was opened after 5 s allowing the mouse to explore the box. The step-through latency was measured up to 300 s.

Sacrifice and brain sampling. Animals were sacrificed on day 11, and their brains were collected. Hippocampus and cortex were isolated and frozen in liquid nitrogen for further evaluation. Brain samples were stored at −80°C.

Statistical analysis. Statistical analysis of weight gain and results from Y-maze assay were performed with GraphPad Prism 5.0 using one-way ANOVA (*F* value), followed by the Dunnett's *post-hoc* multiple comparison test. As passive avoidance latencies have cut-off times after 300 s, the results do not follow a Gaussian distribution. Therefore, they were analyzed using a Kruskal-Wallis non-parametric ANOVA (*H* value), followed by a Dunn's multiple comparison test. $p < 0.05$ was considered as statistically significant.

Associated content

Spectral data for the compounds and uptake experiments can be found in the supporting information.

Author contributions

The manuscript was written through contributions of all authors. All authors have given approval to the final version of the manuscript.

Funding sources

Acknowledgment

Appendix A. Supplementary data

Supplementary data to this article can be found online at https://doi.org/10.1016/j.redox.2019.101378.

Abbreviations

GSH   glutathione
IAA   iodoacetic acid
IL6   interleukin 6
Nrf2   nuclear factor (erythroid-derived 2)-like 2
TNFα   tumor necrosis factor α

References

[1] World Alzheimer report 2018; Alzheimer's disease international, https://www.alz.co.uk/research/world-report-2018 , Accessed date: 31 July 2019.

[2] A.J. Doig, M.P. Del Castillo-Frias, O. Berthoumieu, B. Tarus, J. Nasica-Labouze, F. Sterpone, P.H. Nguyen, N.M. Hooper, P. Faller, P. Derreumaux, Why is research on amyloid-beta failing to give new drugs for Alzheimer's disease? ACS Chem. Neurosci. 8 (7) (2017) 1435–1437.

[3] P. Agostinho, R.A. Cunha, C.N. Oliveira, Oxidative stress and the pathogenesis of Alzheimer's disease, Curr. Pharmaceut. Des. 16 (25) (2010) 2766–2778.

[4] F. Pohl, P. Kong Thoo Lin, The potential use of plant natural products and plant extracts with antioxidant properties for the prevention/treatment of neurodegenerative diseases: in vitro, in vivo and clinical trials, Molecules 23 (12) (2018) 3283–3313.

[5] A. Currais, C. Chiruta, M. Goujon-Svrzic, G. Costa, T. Santos, M.T. Batista, J. Paiva, M. do Ceu Madureira, P. Maher, Screening and identification of neuroprotective compounds relevant to alzheimers disease from medicinal plants of S. Tomé e Príncipe, J. Ethnopharmacol. 155 (1) (2014) 830–840.

[6] S. Schramm, G. Huang, S. Gunesch, F. Lang, J. Roa, P. Högger, R. Sabate, P. Maher, M. Decker, Regioselective synthesis of 7-O-esters of the flavonolignan silibinin and sars lead to compounds with overadditive neuroprotective effects, Eur. J. Med. Chem. 146 (2018) 93–107.

[7] S. Gunesch, S. Schramm, M. Decker, Natural antioxidants in hybrids for the treatment of neurodegenerative diseases: a successful strategy? Future Med. Chem. 9 (8) (2017) 711–713.

[8] J.B. Baell, Feeling nature's pains: natural products, natural product drugs, and pan assay interference compounds (PAINS), J. Nat. Prod. 79 (3) (2016) 616–628.

[9] N.H. Gay, K. Phopin, W. Suwanjang, N. Songtawee, W. Ruankham, P. Wongchitrat, S. Prachayasittikul, V. Prachayasittikul, Neuroprotective effects of phenolic and carboxylic acids on oxidative stress-induced toxicity in human neuroblastoma SH-SY5Y cells, Neurochem. Res. 43 (3) (2018) 619–636.

[10] J.J. Yan, J.Y. Cho, H.S. Kim, K.L. Kim, J.S. Jung, S.O. Huh, H.W. Suh, Y.H. Kim, D.K. Song, Protection against beta-amyloid peptide toxicity in vivo with long-term administration of ferulic acid, Br. J. Pharmacol. 133 (1) (2001) 89–96.

[11] T. Mori, N. Koyama, M.V. Guillot-Sestier, J. Tan, T. Town, Ferulic acid is a nutraceutical beta-secretase modulator that improves behavioral impairment and Alzheimer-like pathology in transgenic mice, PLoS One 8 (2) (2013) e55774.

[12] S. Chakrabarti, M. Jana, A. Roy, K. Pahan, Upregulation of suppressor of cytokine signaling 3 in microglia by cinnamic acid, Curr. Alzheimer Res. 15 (10) (2018) 894–904.

[13] S. Schramm, S. Gunesch, F. Lang, M. Saedtler, L. Meinel, P. Högger, M. Decker, Investigations into neuroprotectivity, stability, and water solubility of 7-O-cinnamoylsilibinin, its hemisuccinate and dehydro derivatives, Arch. Pharm. Chem. Life Sci. 351 (11) (2018).

[14] M. Sato, K. Murakami, M. Uno, Y. Nakagawa, S. Katayama, K. Akagi, Y. Masuda, K. Takegoshi, K. Irie, Site-specific inhibitory mechanism for amyloid beta42 aggregation by catechol-type flavonoids targeting the Lys residues, J. Biol. Chem. 288 (32) (2013) 23212–23224.

[15] T. Ginex, M. Trius, F.J. Luque, Computational study of the aza-Michael addition of the flavonoid (+)-taxifolin in the inhibition of beta-amyloid fibril aggregation, Chem. Eur. J. 24 (22) (2018) 5813–5824.

[16] J. Vrba, R. Gazak, M. Kuzma, B. Papouskova, J. Vacek, M. Weiszenstein, V. Kren, J. Ulrichova, A novel semisynthetic flavonoid 7-O-galloyltaxifolin upregulates heme oxygenase-1 in RAW264.7 cells via MAPK/Nrf2 pathway, J. Med. Chem. 56 (3) (2013) 856–866.

[17] T. Inoue, S. Saito, M. Tanaka, H. Yamakage, T. Kusakabe, A. Shimatsu, M. Ihara, N. Satoh-Asahara, Pleiotropic neuroprotective effects of taxifolin in cerebral amyloid angiopathy, Proc. Natl. Acad. Sci. U.S.A. 116 (20) (2019) 10031–10038.

[18] M. Tanaka, S. Saito, T. Inoue, N. Satoh-Asahara, M. Ihara, Novel therapeutic potentials of taxifolin for amyloid-beta-associated neurodegenerative diseases and other diseases: recent advances and future perspectives, Int. J. Mol. Sci. 20 (9) (2019).

[19] A. Sgarbossa, D. Giacomazza, M. di Carlo, Ferulic acid: a hope for Alzheimer's disease therapy from plants, Nutrients 7 (7) (2015) 5764–5782.

[20] M. Prior, C. Chiruta, A. Currais, J. Goldberg, J. Ramsey, R. Dargusch, P.A. Maher, D. Schubert, Back to the future with phenotypic screening, ACS Chem. Neurosci. 5 (7) (2014) 503–513.

[21] T. Maurice, B.P. Lockhart, A. Privat, Amnesia induced in mice by centrally administered beta-amyloid peptides involves cholinergic dysfunction, Brain Res. 706 (2) (1996) 181–193.

[22] S. Tan, D. Schubert, P. Oxytosis Maher, A novel form of programmed cell death, Curr. Top. Med. Chem. 1 (6) (2001) 497–506.

[23] A. Currais, P. Maher, Functional consequences of age-dependent changes in glutathione status in the brain, Antioxidants Redox Signal. 19 (8) (2013) 813–822.

[24] J. Lewerenz, G. Ates, A. Methner, M. Conrad, P. Maher, Oxytosis/ferroptosis-(re-) emerging roles for oxidative stress-dependent non-apoptotic cell death in diseases of the central nervous system, Front. Neurosci. 12 (214) (2018).

[25] P. Maher, K. van Leyen, P.N. Dey, B. Honrath, A. Dolga, A. Methner, The role of Ca (2+) in cell death caused by oxidative glutamate toxicity and ferroptosis, Cell Calcium 70 (2018) 47–55.

[26] W.S. Yang, K.J. Kim, M.M. Gaschler, M. Patel, M.S. Shchepinov, B.R. Stockwell, Peroxidation of polyunsaturated fatty acids by lipoxygenases drives ferroptosis, Proc. Natl. Acad. Sci. U.S.A. 113 (34) (2016) 4966–4975.

[27] U. Saxena, Bioenergetics failure in neurodegenerative diseases: back to the future, Expert Opin. Ther. Targets 16 (4) (2012) 351–354.

[28] P. Maher, K.F. Salgado, J.A. Zivin, P.A. Lapchak, A novel approach to screening for new neuroprotective compounds for the treatment of stroke, Brain Res. 1173 (2007) 117–125.

[29] T. Wyss-Coray, J. Rogers, Inflammation in Alzheimer disease-a brief review of the basic science and clinical literature, Cold Spring Harbor Perspect. Med. 2 (1) (2012) a006346.

[30] D. Dolles, M. Hoffmann, S. Gunesch, O. Marinelli, J. Moller, G. Santoni, A. Chatonnet, M.J. Lohse, H.J. Wittmann, A. Strasser, M. Nabissi, T. Maurice, M. Decker, Structure-activity relationships and computational investigations into the development of potent and balanced dual-acting butyrylcholinesterase inhibitors and human cannabinoid receptor 2 ligands with pro-cognitive in vivo profiles, J. Med. Chem. 61 (4) (2018) 1646–1663.

[31] V. Lahmy, J. Meunier, S. Malmstrom, G. Naert, L. Givalois, S.H. Kim, V. Villard, A. Vamvakides, T. Maurice, Blockade of tau hyperphosphorylation and Abeta1-42 generation by the aminotetrahydrofuran derivative anavex2-73, a mixed muscarinic and sigma(1) receptor agonist, in a nontransgenic mouse model of Alzheimer's disease, Neuropsychopharmacology 38 (9) (2013) 1706–1723.

[32] M.V. Turovskaya, S.G. Gaidin, V.N. Mal'tseva, V.P. Zinchenko, E.A. Turovsky, Taxifolin protects neurons against ischemic injury in vitro via the activation of antioxidant systems and signal transduction pathways of gabaergic neurons, Mol. Cell. Neurosci. 96 (2019) 10–24.

[33] J.P. Spencer, K. Vafeiadou, R.J. Williams, D. Neuroinflammation Vauzour, Modulation by flavonoids and mechanisms of action, Mol. Asp. Med. 33 (1) (2012) 83–97.

[34] R. Gazak, P. Sedmera, M. Vrbacky, J. Vostalova, Z. Drahota, P. Marhol, D. Walterova, V. Kren, Molecular mechanisms of silybin and 2,3-dehydrosilybin antiradical activity-role of individual hydroxyl groups, Free Radic. Biol. Med. 46 (6) (2009) 745–758.

[35] A. Mattarei, L. Biasutto, F. Rastrelli, S. Garbisa, E. Marotta, M. Zoratti, C. Paradisi, Regioselective O-derivatization of quercetin via ester intermediates. An improved synthesis of rhamnetin and development of a new mitochondriotropic derivative, Molecules 15 (7) (2010) 4722–4736.

[36] R. Gazak, K. Purchartova, P. Marhol, L. Zivna, P. Sedmera, K. Valentova, N. Kato, H. Matsumura, K. Kaihatsu, V. Kren, Antioxidant and antiviral activities of silybin fatty acid conjugates, Eur. J. Med. Chem. 45 (3) (2010) 1059–1067.

[37] D. Schubert, P. Maher, An alternative approach to drug discovery for Alzheimer's disease dementia, Future Med. Chem. 4 (13) (2012) 1681–1688.

[38] J.L. Ehren, P. Maher, Concurrent regulation of the transcription factors Nrf2 and ATF4 mediates the enhancement of glutathione levels by the flavonoid fisetin, Biochem. Pharmacol. 85 (12) (2013) 1816–1826.

[39] N. Ballatori, S.M. Krance, S. Notenboom, S. Shi, K. Tieu, C.L. Hammond, Glutathione dysregulation and the etiology and progression of human diseases, Biol. Chem. 390 (3) (2009) 191–214.

[40] L. Teng, H. Teng, Z. Jia, M. Battino, A. Miron, Z. Yu, H. Cao, J. Xiao, Intracellular signaling pathways of inflammation modulated by dietary flavonoids: the most recent evidence, Crit. Rev. Food Sci. Nutr. 58 (17) (2018) 2908–2924.

[41] E.H. Kobayashi, T. Suzuki, R. Funayama, T. Nagashima, M. Hayashi, H. Sekine, N. Tanaka, T. Moriguchi, H. Motohashi, K. Nakayama, M. Yamamoto, Nrf2 suppresses macrophage inflammatory response by blocking proinflammatory cytokine transcription, Nat. Commun. 7 (2016) 11624–11638.

[42] P. Lu, T. Mamiya, L.L. Lu, A. Mouri, L. Zou, T. Nagai, M. Hiramatsu, T. Ikejima, T. Nabeshima, Silibinin prevents amyloid beta peptide-induced memory impairment and oxidative stress in mice, Br. J. Pharmacol. 157 (7) (2009) 1270–1277.

[43] X. Song, B. Zhou, P. Zhang, D. Lei, Y. Wang, G. Yao, T. Hayashi, M. Xia, S. Tashiro, S. Onodera, T. Ikejima, Protective effect of silibinin on learning and memory impairment in LPS-treated rats via ROS-BDNF-TrkB pathway, Neurochem. Res. 41 (7) (2016) 1662–1672.

[44] K. Yamada, T. Tanaka, D. Han, K. Senzaki, T. Kameyama, T. Nabeshima, Protective effects of idebenone and alpha-tocopherol on beta-amyloid-(1-42)-induced learning

and memory deficits in rats: implication of oxidative stress in beta-amyloid-induced neurotoxicity in vivo, Eur. J. Neurosci. 11 (1) (1999) 83–90.

[45] Y. Wang, Q. Wang, X. Bao, Y. Ding, J. Shentu, W. Cui, X. Chen, X. Wei, S. Xu, Taxifolin prevents beta-amyloid-induced impairments of synaptic formation and deficits of memory via the inhibition of cytosolic phospholipase A$_2$/prostaglandin E$_2$ content, Metab. Brain Dis. 33 (4) (2018) 1069–1079.

[46] S.Y. Park, H.Y. Kim, H.J. Park, H.K. Shin, K.W. Hong, C.D. Kim, Concurrent treatment with taxifolin and cilostazol on the lowering of beta-amyloid accumulation and neurotoxicity via the suppression of P-JAK2/P-STAT3/NF-kappaB/BACE1 signaling pathways, PLoS One 11 (12) (2016) e0168286.

[47] J. Meunier, V. Villard, L. Givalois, T. Maurice, The gamma-secretase inhibitor 2-[(1r)-1-[(4-chlorophenyl)sulfonyl](2,5-difluorophenyl) amino]ethyl-5-fluor-obenzenebutanoic acid (BMS-299897) alleviates Abeta1-42 seeding and short-term memory deficits in the Abeta25-35 mouse model of Alzheimer's disease, Eur. J. Pharmacol. 698 (1–3) (2013) 193–199.

[48] S. Saito, Y. Yamamoto, T. Maki, Y. Hattori, H. Ito, K. Mizuno, M. Harada-Shiba, R.N. Kalaria, M. Fukushima, R. Takahashi, M. Ihara, Taxifolin inhibits amyloid-beta oligomer formation and fully restores vascular integrity and memory in cerebral amyloid angiopathy, Acta Neuropathol. Commun. 5 (26) (2017).

[49] P. Maher, Potentiation of glutathione loss and nerve cell death by the transition metals iron and copper: implications for age-related neurodegenerative diseases, Free Radic. Biol. Med. 115 (2018) 92–104.

[50] T. Maurice, M. Strehaiano, N. Simeon, C. Bertrand, A. Chatonnet, Learning performances and vulnerability to amyloid toxicity in the butyrylcholinesterase knockout mouse, Behav. Brain Res. 296 (2016) 351–360.